Adaptive Dual-Layer Super-Twisting Sliding Mode Observers to Reconstruct and Mitigate Disturbances and Communication Attacks in Power Networks

Gianmario Rinaldi[1], Prathyush P. Menon[1], Christopher Edwards[1], Antonella Ferrara[2], Yuri Shtessel[3]

[1] *College of Engineering, Mathematics, and Physical Sciences, University of Exeter, Exeter, United Kingdom*

[2] *Department of Electrical, Computer and Biomedical Engineering, University of Pavia, Pavia, Italy*

[3] *University of Alabama in Huntsville, Huntsville, Alabama, USA*

Abstract

In this paper a novel distributed adaptive dual-layer super-twisting sliding mode observer-based scheme is designed to isolate, reconstruct and mitigate the effects of disturbances and a class of communication attacks affecting both generator nodes and load nodes in power networks. Voltage phase angles are measured at each node by means of Phasor Measurement Units (PMUs). Based on this information, an interconnection of adaptive dual-layer super-twisting sliding mode observers is designed both to estimate frequency deviation in each generator node, and to perform robust detection and reconstruction of both disturbances and a class of communication attacks. The proposed estimation scheme exhibits a distributed structure, since it requires only information received from neighbouring nodes and measurements taken locally in the power network. The novelty of the proposed scheme is its capability to reconstruct simultaneous disturbances affecting the generator nodes and load nodes, automatically adjusting the values of the gains of the observers. More precisely, the adaptive gains of the observer obey a recently proposed dual-layer adaptation law for the super-twisting sliding mode architecture. A disturbance mitigation strategy is also proposed at each generator node utilising the disturbance estimates. Numerical simulations are discussed to assess the proposed distributed scheme.

Keywords: Sliding mode; Observers; Power systems; Large-scale-system; State estimation; Fault detection; Fault isolation.

1. Introduction

The rapid expansion of novel heterogeneous renewable energy based sources, and increasing power demands are causing new issues and challenges in power systems (Tsai et al., 2017). Phasor Measurement Units (PMUs) have been recently proposed to provide synchronized faster measurements of real-time voltages and currents (Phadke and Thorp, 2017). By making use of the measurements gathered from PMUs, it is now possible to design more accurate, robust and dynamic state estimators (Tebianian and Jeyasurya, 2015), (Rinaldi et al., 2018b), (Pasqualetti et al., 2015). The timely and accurate isolation and reconstruction of disturbances and attacks can then be exploited to attenuate their impact on the stability of the power system (Wang and Lu, 2013). Faults can also degrade the performances of conventional frequency controllers for synchronous generators. A state-of-the-art review of conventional and more innovative frequency control approaches can be found, for example, in Shayeghi et al. (2009). Perhaps, unsurprisingly, Proportional Integral (PI) controllers represent the most common approach implemented in practice (Pappachen and Fathima, 2017). In the literature, relatively few relevant papers have proposed approaches to isolate and reconstruct disturbances in power grids. In Saoudi and Harmas (2014) an adaptive fuzzy sliding mode-based scheme has been

Email addresses: gr344@exeter.ac.uk (Gianmario Rinaldi[1]), P.M.Prathyush@exeter.ac.uk (Prathyush P. Menon[1]), C.Edwards@exeter.ac.uk (Christopher Edwards[1]), antonella.ferrara@unipv.it (Antonella Ferrara[2]), shtessy@uah.edu (Yuri Shtessel[3])

employed to stabilise multi-machine power systems in the presence of disturbances, combining a proportional integral controller with a sliding mode controller. More recently, in Rinaldi et al. (2020), a robust sliding mode observer has been designed to detect and reconstruct state and output attacks for a linearised differential-algebraic model of a power network, whilst in Rinaldi et al. (2017), third order sliding mode observers have been proposed to dynamically reconstruct frequency deviation and power governor variation in a network of thermal power plants subjected to bounded disturbances. More recently, in Nateghi et al. (2019) secure sliding mode observer-based state estimation has been proposed to deal with corrupted states and measurements. The proposed approaches revealed to be completely centralised and applied to the linearised IEEE 14 bus benchmark.

A distributed observer-based adaptive control method has been proposed in Shi and Shen (2017) to achieve leader-following consensus in multi-agent uncertain systems. More recently, in Shen et al. (2019a) an adaptive fuzzy control methodology has been conceived to ensure that the tracking error converges to an adjustable small neighbourhood of the origin. In Shen et al. (2019b) the consensus problem of a class of leader-following systems on undirected graph with a fixed topology has been addressed via adaptive controllers.

Adaptive sliding mode estimators have been exploited in relatively few relevant works. For example, in Liu et al. (2014) an adaptive-gain second order sliding mode observer has been employed for multi-cell converters. In Tursini et al. (2000) an adaptive first order sliding mode observer has been used to estimate the rotor flux component for the purpose of speed control in induction motors. Similarly, in Li et al. (2005) two sliding-mode observers have been employed with application to induction motors to make flux and speed estimation robust to parameter variations.

In this paper a novel distributed adaptive dual-layer super-twisting sliding mode observer is presented. The proposed observation approach enables to isolate, reconstruct and mitigate the effects of the disturbances, as well as a class of communication attacks affecting both generator nodes and load nodes in power networks. The adaptive gains of the observer are self-tuned in accordance with the dual-layer adaptation algorithm recently introduced Edwards and Shtessel (2016). If accurate upper bounds on the uncertainties are represented by known nonlinear functions of the states, the variable gains super-twisting approach in Gonzalez et al. (2011) could be used. Similar to Edwards and Shtessel (2016) and to Moreno et al. (2016) we assumed very little knowledge of the uncertainties, and the gains of the super-twisting scheme are functions of an adapting parameter depending on the output observation error. However, whereas in Moreno et al. (2016) the changing parameter is monotonically increasing until sliding motion is established, in our paper the mechanism for adapting the gains is based on the "dual layer" work of Edwards and Shtessel (2016) and guarantees that if sliding is lost, in finite time, the gain is sufficiently increased until sliding is restored. Another beneficial feature of the adopted methodology is that during sliding, the adaptive gain takes as small as possible value to maintain sliding. Again, similarly to Edwards and Shtessel (2016), in the present paper, the values of the observer adaptive gains are increasing in a concert prior to achieving the second order sliding mode (2-SM). The adaptive gain values dynamically respond to the changes in the disturbance profiles and attempt to decrease when the disturbance decreases.

Main Contribution

The main contribution of the present paper is the design of a distributed scheme based on an adaptive dual-layer super-twisting sliding mode architecture to perform robust disturbance and communication attack reconstruction and mitigation in power systems. In the present paper, multiple disturbances and communication attacks affecting generators and loads are considered. The starting point of the present work can be considered to be Rinaldi et al. (2018a), but several novelties are provided in contrast to the earlier work:

- The dynamical model for the power system is nonlinear and it comprises frequency-dependent load dynamics (Zhao et al., 2015), which makes the approach closer to the real practice.
- In our paper the mechanism for adapting the gains is directly the "dual layer" work of Edwards and Shtessel (2016) and guarantees that if sliding is broken, in finite time, the gain is sufficiently increased until sliding is restored. It follows that it is no longer necessary to know a priori a value for the upper-bounds of the disturbances. During sliding the adaptive gain seeks to take as small as possible a value to maintain sliding. This helps mitigating chattering and the amplification of noise.

Table 1: List of Symbols and Variables Used in the Paper.

Symbol	Meaning
δ_i (rad)	generator voltage phase angle
$\Delta\omega_{g_i}$ (p.u.)	generator frequency deviation
ϑ_i (rad)	load voltage phase angle
$\Delta\omega_{l_i}$ (p.u.)	load frequency deviation
P_{g_i} (p.u.)	generator input power
P_{l_i} (p.u.)	load power demand
f_{g_i} (p.u.)	disturbance acting on a generator
f_{l_i} (p.u.)	disturbance acting on a load
D_{g_i} (p.u.)	generator droop control coefficient
D_{l_i} (p.u.)	load droop control coefficient
M_i (p.u.)	generator inertia
B_{ij} (p.u.)	transmission line susceptance

- A class of communication attacks amongst the observers is tackled. Moreover, here it will be shown that a standard pre-existing Proportional Integral (PI) controller can still be employed (Kundur et al., 1994), suitably coupled with disturbance compensation.

Numerical simulations, which are based on the IEEE 39 bus power network (Hiskens, 2013), are used to assess the proposed estimation technique. To the best of the authors' knowledge, the use of a network of adaptive dual-layer super-twisting sliding mode observers, applied to isolate and reconstruct multiple disturbances and communication attacks on generators and/or on loads in power networks, has never been proposed before.

2. Power Network System Description

2.1. Graph Theory Recalls

A power network can be interpreted as a connected and undirected graph $G(\mathcal{N},\mathcal{E})$, including the set of nodes $\mathcal{N}$ (which are associated with the generators and the loads), and the set of edges $\mathcal{E}$ (which represents the power transmission lines) (Dorfler and Bullo, 2013). The set of node $\mathcal{N}$ is partitioned into the set of generators $\mathcal{G}$ and the set of edges $\mathcal{L}$ such that $\mathcal{N} = \mathcal{G} \cup \mathcal{L}$. The weight B_{ij} (which is the susceptance) characterizes the edge between the i-th and the j-th node. The set $\mathcal{N}_i$ is the neighborhood of the i-th node and can be decomposed into the neighboring generator nodes set $\mathcal{M}_i$, and the neighboring load nodes set $\mathcal{O}_i$, such that $\mathcal{N}_i = \mathcal{M}_i \cup \mathcal{O}_i$.

2.2. Generator Dynamics

The following differential equations describe the dynamics of each generator node (Kundur et al., 1994):

$$\begin{array}{rcl} \dot{\delta}_i & = & \Delta\omega_{g_i} \\ M_i\Delta\dot{\omega}_{g_i} & = & P_{g_i} - D_{g_i}\Delta\omega_{g_i} - \sum_{j\in\mathcal{N}_i} B_{ij}\sin(\delta_i - \vartheta_j) + f_{g_i} \\ y_{g_i} & = & \delta_i. \end{array} \tag{1}$$

The reader is referred to Table 1 for the description of the state variables for the generators (δ_i, $\Delta\omega_{g_i}$), for the known input (P_{g_i}) and the model parameters. In (1), the expression $-\sum_{j\in\mathcal{N}_i} B_{ij}\sin(\delta_i - \vartheta_j)$ denotes the total electrical active power flowing from the i-th generator node to its neighbourhood (Sauer et al., 2017), while f_{g_i} is a disturbance that can act on the i-th generator node. The only output measured by a PMU (Phadke and Thorp, 2017) is the generator voltage phase angle $y_{g_i} = \delta_i$.

2.3. Load Dynamics

The so-called frequency-dependent load dynamical model is adopted in the present work (Kundur et al., 1994). Specifically, the following differential-algebraic structure will be used

$$\begin{array}{rcl} \dot{\vartheta}_i & = & \Delta\omega_{l_i} \\ 0 & = & P_{l_i} - D_{l_i}\Delta\omega_{l_i} - \sum_{j\in\mathcal{M}_i} B_{ij}\sin(\vartheta_i - \delta_j) - \sum_{k\in\mathcal{O}_i} B_{ik}\sin(\vartheta_i - \vartheta_k) + f_{l_i} \\ y_{l_i} & = & \vartheta_i. \end{array} \tag{2}$$

The system in equation (2) can be rewritten as a single differential equation:

$$\begin{array}{rcl} D_{l_i}\dot{\vartheta}_i & = & P_{l_i} - \sum_{j\in\mathcal{M}_i} B_{ij}\sin(\vartheta_i-\delta_j) - \sum_{k\in\mathcal{O}_i} B_{ik}\sin(\vartheta_i-\vartheta_k) + f_{l_i} \\ y_{l_i} & = & \vartheta_i. \end{array} \tag{3}$$

Table 1 describes the state variables for the load (ϑ_i), the known input $\left(P_{l_i}\right)$ and the model parameters. The only output measurement is the load voltage phase angle $y_{l_i} = \vartheta_i$ gathered from a PMU.

For both the generator and the load dynamics, the following assumption is imposed:

Assumption 1. *It is assumed that:*

(A1) The model parameters in (1) *and in* (3) *are assumed to be locally known at the i-th generator and at the i-th load level, respectively.*

(A2) Signal f_{g_i} in (1) *is a bounded differentiable disturbance. The bounds for the disturbance itself and for its time derivative are assumed to be finite but unknown. It follows that $|f_{g_i}| < \lambda_{1_{g_i}}$, $|\dot{f}_{g_i}| < \lambda_{2_{g_i}}$, where $\lambda_{1_{g_i}}$, $\lambda_{2_{g_i}}$ are positive unknown constants.*

(A3) Signal f_{l_i} in (3) *is a twice bounded differentiable disturbance. The bounds for the disturbance itself and for its first and second time derivatives are assumed to be finite but unknown. It follows that $|f_{l_i}| < \lambda_{1_{l_i}}$, $|\dot{f}_{l_i}| < \lambda_{2_{l_i}}$, and $|\ddot{f}_{l_i}| < \lambda_{3_{l_i}}$ where $\lambda_{1_{l_i}}$, $\lambda_{2_{l_i}}$, and $\lambda_{3_{l_i}}$ are positive unknown constants.*

3. Adaptive Observers Design

3.1. Generator Observer

The following adaptive super-twisting-like sliding mode observer is proposed to estimate the frequency deviation in each generator node, exploiting ideas from Rinaldi et al. (2020) and from Edwards and Shtessel (2016)[1]:

$$\begin{array}{rcl} \dot{\hat{\delta}}_i & = & -\alpha_i(t)\left|e_{\delta_i}\right|^{1/2}\mathrm{sign}\left(e_{\delta_i}\right) - a_i e_{\delta_i} + \Delta\hat{\omega}_{g_i} + \Phi_{g_i}\left(L_{g_i}(t), e_{\delta_i}\right) \\ \Delta\dot{\hat{\omega}}_{g_i} & = & \frac{1}{M_i}\Big(P_{g_i} - D_{g_i}\Delta\hat{\omega}_{g_i} - \sum_{j\in\mathcal{N}_i} B_{ij}\sin\left(y_{g_i}-y_{l_j}\right)\Big) \\ & & -\beta_i(t)\mathrm{sign}\left(e_{\delta_i}\right) - a_i^2 e_{\delta_i} + a_i\Phi_{g_i}\left(L_{g_i}(t), e_{\delta_i}\right) \\ & & -a_i\alpha_i(t)\left|e_{\delta_i}\right|^{1/2}\mathrm{sign}\left(e_{\delta_i}\right) \qquad (4) \\ \hat{y}_{g_i} & = & \hat{\delta}_i, \qquad (5) \end{array}$$

where $\hat{\delta}_i$ is the estimate of δ_i, $\Delta\hat{\omega}_{g_i}$ is the estimate of $\Delta\omega_{g_i}$, $e_{\delta_i} \triangleq \hat{\delta}_i - \delta_i$, $a_i \triangleq -D_{g_i}/M_i$, whilst $\alpha_i(t)$ and $\beta_i(t)$ are time-varying gains. The terms $\Phi_{g_i}(\cdot)$ and $L_{g_i}(t)$ are additional terms driven by the output estimation error and will be described in the sequel.

Remark 1. *In* (4)*, an additional term $-a_i e_{\delta_i}$ is present compared to the adaptive super-twisting approach in Edwards and Shtessel (2016), whilst in* (4) *$-a_i^2 e_{\delta_i}$, $-a_i\alpha_i(t)\left|e_{\delta_i}\right|^{1/2}\mathrm{sign}\left(e_{\delta_i}\right)$, and $a_i\Phi_{g_i}\left(L_{g_i}(t), e_{\delta_i}\right)$ have been included. The motivation for these choices is detailed in the sequel. In addition, in contrast to Rinaldi et al. (2020), the observer exploits measurements of the voltage phase angles y_{l_j} from the neighbouring load nodes, gathered by PMUs.*

[1] The time dependence on the variable is reported from this point onwards on the paper only for the time-varying gains of the observers and for the auxiliary signals for the implementation of the adaptation law.

By subtracting (4)-(4) from (1), one obtains

$$\begin{aligned}\dot{e}_{\delta_i} &= -\alpha_i(t)|e_{\delta_i}|^{1/2}\text{sign}\left(e_{\delta_i}\right) \\ &\quad -a_i e_{\delta_i} + e_{\omega_i} + \Phi_{g_i}\left(L_{g_i}(t), e_{\delta_i}\right) \qquad (6)\\ \dot{e}_{\omega_i} &= -a_i\alpha_i(t)\left|e_{\delta_i}\right|^{1/2}\text{sign}\left(e_{\delta_i}\right) + a_i\Phi_{g_i}\left(L_{g_i}(t), e_{\delta_i}\right) \\ &\quad +a_i e_{\omega_i} - \beta_i(t)\text{sign}\left(e_{\delta_i}\right) - a_i^2 e_{\delta_i} - \frac{f_{g_i}}{M_i}, \qquad (7)\end{aligned}$$

where $e_{\omega_i} \triangleq \Delta\hat{\omega}_{g_i} - \Delta\omega_{g_i}$. Exploiting ideas from Edwards and Shtessel (2016), the following time-varying gains are chosen

$$\begin{aligned}\alpha_i(t) &= \sqrt{L_{g_i}(t)}\alpha_{0_i} \qquad (8)\\ \beta_i(t) &= L_{g_i}(t)\beta_{0_i}, \qquad (9)\end{aligned}$$

where α_{0_i} and β_{0_i} are positive constants. The time varying positive gain $L_{g_i}(t)$ is selected as follows

$$L_{g_i}(t) = l_{0_i} + l_{g_i}(t), \qquad (10)$$

where l_{0_i} is a positive constant and $l_{g_i}(t)$ satisfies the adaptation law

$$\dot{l}_{g_i}(t) = -\rho_{g_i}(t)\text{sign}\left(\varphi_{g_i}(t)\right). \qquad (11)$$

where the quantity $\varphi_{g_i}(t)$ will be defined later. The additional nonlinear term $\Phi_{g_i}(\cdot)$ is selected as

$$\Phi_{g_i}\left(L_{g_i}(t), e_{\delta_i}\right) = -\frac{\dot{L}_{g_i}(t)}{L_{g_i}(t)}e_{\delta_i}. \qquad (12)$$

In (11), the time-varying scalar $\rho_{g_i}(t)$ is given by

$$\rho_{g_i}(t) = r_{0_i} + r_{g_i}(t), \qquad (13)$$

where r_{0_i} is a positive design constant and $r_{g_i}(t)$ satisfies

$$\dot{r}_{g_i}(t) = \gamma_i\left|\varphi_{g_i}(t)\right|, \qquad (14)$$

where γ_i is a positive design constant. The signal $\varphi_{g_i}(t)$ in (11) and (14) is defined as

$$\varphi_{g_i}(t) = L_{g_i}(t) - \frac{1}{\eta_i\beta_{0_i}}\left|v_{g_i}(t)\right| - \iota_{g_i}, \qquad (15)$$

where the constant η_i is chosen such that $0 < \eta_i < 1/\beta_{0_i} < 1$, whilst ι_{g_i} satisfies

$$\frac{1}{\eta_i\beta_{0_i}}\left|v_{g_i}(t)\right| + \frac{\iota_{g_i}}{2} > \left|v_{g_i}(t)\right| \qquad (16)$$

Finally, signal $v_{g_i}(t)$ represents an approximation of the equivalent injection associated with the discontinuous signal $\beta_i(t)\text{sign}\left(e_{\delta_i}\right)$ in (4), and is generated from a low-pass filter: here

$$\dot{v}_{g_i}(t) = \frac{1}{\tau_i}\left(\beta_i(t)\text{sign}\left(e_{\delta_i}\right) - v_{g_i}(t)\right), \qquad (17)$$

where τ_i is a small positive constant known in advance and selected based on engineering intuition about the system. By defining the variable $\bar{e}_{\omega_i} = e_{\omega_i} - a_i e_{\delta_i}$, the system of equations (6)-(7) can be rewritten as follows

$$\begin{aligned}
\dot{e}_{\delta_i} &= -\alpha_i(t)|e_{\delta_i}|^{1/2}\text{sign}\big(e_{\delta_i}\big)+\bar{e}_{\omega_i}+\Phi_{g_i}\big(L_{g_i}(t),e_{\delta_i}\big) \\
\dot{\bar{e}}_{\omega_i} &= a_i e_{\omega_i} - \beta_i(t)\text{sign}\left(e_{\delta_i}\right) - a_i^2 e_{\delta_i} \\
&\quad -a_i\alpha_i(t)\left|e_{\delta_i}\right|^{1/2}\text{sign}\left(e_{\delta_i}\right) - \frac{f_{g_i}}{M_i} \\
&\quad +a_i\Phi_{g_i}\big(L_{g_i}(t),e_{\delta_i}\big) - a_i\big(e_{\omega_i} - a_i e_{\delta_i} \\
&\quad -\alpha_i(t)|e_{\delta_i}|^{1/2}\text{sign}\left(e_{\delta_i}\right) + \Phi_{g_i}\left(L_{g_i}(t),e_{\delta_i}\right)\big)
\end{aligned} \tag{18}$$

After straightforward algebraic manipulations

$$\begin{aligned}
\dot{e}_{\delta_i} &= \bar{e}_{\omega_i} - \alpha_i(t)|e_{\delta_i}|^{1/2}\text{sign}\big(e_{\delta_i}\big)+\Phi_{g_i}\big(L_{g_i}(t),e_{\delta_i}\big) \\
\dot{\bar{e}}_{\omega_i} &= -\beta_i(t)\text{sign}\left(e_{\delta_i}\right) - \frac{f_{g_i}}{M_i}.
\end{aligned} \tag{19}$$

The following two propositions will now be proven:

Proposition 1. *Choosing*

$$\alpha_{0_i} = 2\sqrt{2}\beta_{0_i} \tag{20}$$

where $\beta_{0_i} > 1$ *and ensuring that*

$$L_{g_i}(t) \geq \max\left\{l_{0_i}, |f_{g_i}|/M_i\right\} \tag{21}$$

the time-varying gains in (8) *and* (9) *guarantee a a second order sliding mode* $e_{\delta_i} = \dot{e}_{\delta_i} = 0$ *in* (19) *in finite time.*

PROOF. See Appendix A. □

Furthermore,

Proposition 2. *Provided that* $|f_{g_i}|$ *and* $|\dot{f}_{g_i}|$ *are bounded (Assumption 1), the dual layer adaptation scheme from* (11) *and* (14) *guarantees that*

$$L_{g_i}(t) > |f_{g_i}|/M_i \tag{22}$$

in finite time.

PROOF. See Appendix B. □

The sliding motion in system (19) is characterised by the conditions $e_{\delta_i} = \dot{e}_{\delta_i} = 0$. The average value v_{g_i} of the discontinuous signal $\beta_i(t)\text{sign}\left(e_{\delta_i}\right)$ compensates for the signal $-f_{g_i}/M_i$ and therefore during the sliding motion

$$v_{g_i} = -\frac{f_{g_i}}{M_i}. \tag{23}$$

An estimation $\hat{f}_{g_i}$ for the disturbance f_{g_i} is given by

$$\hat{f}_{g_i} = -M_i v_{g_i}. \tag{24}$$

Remark 2. *A low-pass filter (Edwards and Spurgeon, 1998) (governed by* (17)*) can be used to extract the signal* v_{g_i} *from the discontinuous signal* $\beta_i(t)\text{sign}\left(e_{\delta_i}\right)$. *The choice of the bandwidth of the filter used to estimate the equivalent injection is really important. The bandwidth must be sufficiently large so the key-frequency components of the*

disturbances are captured, but not too large so that possible noise becomes part of the injection signal. Practically speaking, also the performance and limitations of the software and hardware on which this scheme is implemented must be taken into account. During the tuning process the signal v_{g_i} can be examined, relying on an engineering intuition, to determine whether it represents a meaningful disturbance based on existing statistics of the disturbances and bandwidths of the possible uncertainty.

A disturbance isolation procedure can be easily implemented whenever the modulus of $\hat{f}_{g_i}$ passes an appropriate positive small threshold ε_{g_i}. Specifically

$$\begin{cases} |\hat{f}_{g_i}| \geq \varepsilon_{g_i} & \text{i-th generator node is disturbed} \\ |\hat{f}_{g_i}| < \varepsilon_{g_i} & \text{no disturbance.} \end{cases} \tag{25}$$

Remark 3. *The proposed distributed estimator for a disturbance in one generator node is totally insensitive to other simultaneous disturbances in other (generator or load) nodes. This can be understood by considering the dynamical coupling between the nodes in the power network. This takes place at the voltage phase angle level (see equations* (1) *and* (3)*), which are measured by neighboring PMUs and communicated as stated above.*

3.2. Load Observer

Next consider the following adaptive super-twisting sliding mode observer to estimate disturbances in each load node

$$\begin{aligned} \dot{\hat{\vartheta}}_i &= \frac{1}{D_{l_i}}\Big(P_{l_i} - \sum_{j\in\mathcal{M}_i} B_{ij}\sin\left(y_{l_i} - y_{g_j}\right) \\ &\quad - \sum_{k\in\mathcal{O}_i} B_{ik}\sin\left(y_{l_i} - y_{l_k}\right)\Big) - \lambda_i(t)\left|e_{\vartheta_i}\right|^{1/2}\mathrm{sign}\left(e_{\vartheta_i}\right) \\ &\quad + \hat{\psi}_i + \Phi_{l_i}(L_{l_i}, e_{\vartheta_i}) \\ \dot{\hat{\psi}}_i &= -\mu_i(t)\mathrm{sign}\left(e_{\vartheta_i}\right) \\ \hat{y}_{l_i} &= \hat{\vartheta}_i, \end{aligned} \tag{26}$$

where $\hat{\vartheta}_i$ represents the estimate of ϑ_i, $\hat{\psi}_i$ is an auxiliary state variable, $e_{\vartheta_i} \triangleq \hat{\vartheta}_i - \vartheta_i$, λ_i and μ_i are time-varying gains, and the additional term $\Phi_{l_i}(\cdot)$ is selected analogously to (12). The observer in (26) receives both the measurements of the voltage phase angles y_{g_j} of the neighbouring generator nodes, and the measurements of the voltage phase angles y_{l_k} of the neighbouring load nodes. By defining the new variable

$$e_{\psi_i} \triangleq \hat{\psi}_i - \frac{f_{l_i}}{D_{l_i}}, \tag{27}$$

the error dynamics for the adaptive super-twisting load observer are obtained by subtracting (3) (divided by D_{l_i}) from (26):

$$\begin{aligned} \dot{e}_{\vartheta_i} &= -\lambda_i(t)\left|e_{\vartheta_i}\right|^{1/2}\mathrm{sign}\left(e_{\vartheta_i}\right) + e_{\psi_i} + \Phi_{l_i}\left(L_{l_i}, e_{\vartheta_i}\right) \\ \dot{e}_{\psi_i} &= -\mu_i(t)\mathrm{sign}\left(e_{\vartheta_i}\right) - \frac{\dot{f}_{l_i}}{D_{l_i}}. \end{aligned} \tag{28}$$

Analogously to the error dynamics (19), exploiting again Assumption 1, the system in equation (28) is driven to the origin in a finite time. The sliding motion of the system in (28) is characterised by the conditions $e_{\vartheta_i} = e_{\psi_i} = 0$. Since e_{ψ_i} is steered to zero in a finite time, exploiting its definition in (27), which holds for any time instant, it is apparent that the condition

$$\hat{f}_{l_i} = D_{l_i}\hat{\psi}_i \tag{29}$$

holds in a finite time. From (29) it is apparent that an estimate $\hat{f}_{l_i}$ of the load disturbance f_{l_i} can be obtained.

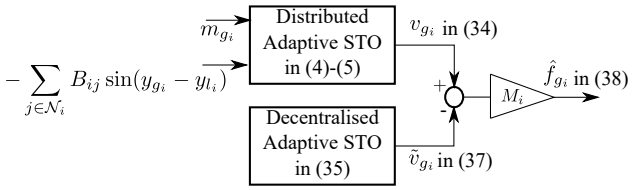

Figure 1: A schematic of the distributed adaptive Super Twisting Observer (STO) in equations (4)-(4), suitably coupled with the additional decentralized STO in (34), for the purpose of disturbance reconstruction in presence of the communication attack $m_{g_i}(t)$.

Remark 4. *In contrast to Remark 2, the low-pass filter is not required to reconstruct the load disturbance, since the signal $\hat{\psi}_i$ is continuous.*

Analogously to (25), the following (practical) criteria for local load disturbance isolation can be adopted

$$\begin{cases} |\hat{f}_{l_i}| \geq \varepsilon_{l_i} & i\text{-th load node is disturbed} \\ |\hat{f}_{l_i}| < \varepsilon_{l_i} & \text{no disturbance,} \end{cases} \tag{30}$$

where ε_{l_i} is an appropriate positive small threshold.

4. Communication Attack Reconstruction

In this section, a class of attacks is assumed to potentially take place at the adaptive super-twisting observers level. More precisely, it is assumed that each observer receives corrupted measurements gathered from the neighbouring nodes and an the effect of the disturbance is cancelled throughout an injection of an attack signal. It will be shown that these kinds of attacks can be isolated and reconstructed by introducing an additional decentralized adaptive super-twisting observer for each node of the power network.

4.1. Generator Observer Communication Attacks Reconstruction

Suppose that each adaptive super-twisting-like sliding mode observer for the generator in the form of (4)-(4) receives the corrupted measurements gathered by the neighbouring nodes and an attack cancelling the effect of the disturbance in its matched channel. This means that signal m_{g_i}, defined as

$$m_{g_i} \triangleq \frac{f_{g_i} + \sum_{j\in\mathcal{N}_i} B_{ij}\sin\left(y_{g_i} - y_{l_j}\right)}{M_i}, \tag{31}$$

will be included in equation (4). By making use of (31), the corrupted observer error dynamics (19) become

$$\begin{aligned} \dot{e}_{\delta_i} &= \bar{e}_{\omega_i} - \alpha_i(t)|e_{\delta_i}|^{1/2}\text{sign}(e_{\delta_i}) + \Phi_{g_i}\left(L_{g_i}(t), e_{\delta_i}\right) \\ \dot{\bar{e}}_{\omega_i} &= -\beta_i(t)\text{sign}\left(e_{\delta_i}\right) \\ &\quad + \frac{\sum_{j\in\mathcal{N}_i} B_{ij}\sin\left(\delta_i - \vartheta_j\right)}{M_i}. \end{aligned} \tag{32}$$

The effect of the bounded disturbance m_{g_i} appears in the matched channel of the system (32), which converges to the origin in a finite time as proved in Section 3. Moreover, equation (23) becomes

$$v_{g_i} = \frac{\sum_{j\in\mathcal{N}_i} B_{ij}\sin\left(\delta_i - \vartheta_j\right)}{M_i}. \tag{33}$$

From (33) it is no longer possible to reconstruct the generator disturbance f_{g_i}, since its effect has been cancelled by (31). In order to solve this issue, an additional decentralised adaptive-super-twisting-like sliding mode observer for

each generator node is introduced:

$$\begin{aligned}
\dot{\tilde{\delta}}_i &= -\tilde{\alpha}_i(t)\left|\tilde{e}_{\delta_i}\right|^{1/2}\text{sign}\left(\tilde{e}_{\delta_i}\right) \\
&\quad -a_i\tilde{e}_{\delta_i}+\Delta\tilde{\omega}_{g_i}+\tilde{\Phi}_{g_i}\left(\tilde{L}_{g_i}(t),\tilde{e}_{\delta_i}\right) \\
\Delta\dot{\tilde{\omega}}_{g_i} &= \frac{1}{M_i}\Big(P_{g_i}-D_{g_i}\Delta\tilde{\omega}_{g_i}\Big) \\
&\quad -\tilde{\beta}_i(t)\text{sign}\left(\tilde{e}_{\delta_i}\right)-a_i^2\tilde{e}_{\delta_i}+a_i\tilde{\Phi}_{g_i}\big(\tilde{L}_{g_i}(t),\tilde{e}_{\delta_i}\big) \\
&\quad -a_i\tilde{\alpha}_i\left|\tilde{e}_{\delta_i}\right|^{1/2}\text{sign}\left(\tilde{e}_{\delta_i}\right) \\
\tilde{y}_{g_i} &= \tilde{\delta}_i,
\end{aligned} \tag{34}$$

where $\tilde{\delta}_i$ denotes now an additional estimate of δ_i, $\Delta\tilde{\omega}_{g_i}$ denotes an additional estimate of $\Delta\omega_{g_i}$, $\tilde{e}_{\delta_i} \triangleq \tilde{\delta}_i - \delta_i$, while $\tilde{\alpha}_i$, $\tilde{\beta}_i$, and $\tilde{\Phi}_{g_i}(\cdot)$ are selected as in Section 3. Exploiting the ideas in Section 3, the error dynamics for the i-th decentralized observer are given by

$$\begin{aligned}
\dot{\tilde{e}}_{\delta_i} &= \tilde{e}_{\omega_i}-\tilde{\alpha}_i(t)\tilde{e}_{\delta_i}|^{1/2}\text{sign}\left(\tilde{e}_{\delta_i}\right)+\tilde{\Phi}_{g_i}\big(\tilde{L}_{g_i}(t),\tilde{e}_{\delta_i}\big) \\
\dot{\tilde{e}}_{\omega_i} &= -\tilde{\beta}_i(t)\text{sign}\left(\tilde{e}_{\delta_i}\right)-\frac{f_{g_i}}{M_i} \\
&\quad +\frac{\sum_{j\in\mathcal{N}_i}B_{ij}\sin\left(\delta_i-\vartheta_j\right)}{M_i},
\end{aligned} \tag{35}$$

which converge to the origin in a finite time as previously. Now the average value $\tilde{v}_{g_i}$ of the discontinuous signal $\tilde{\beta}_i(t)\text{sign}\left(\tilde{e}_{\delta_i}\right)$ satisfies

$$\tilde{v}_{g_i}=\frac{-f_{g_i}+\sum_{j\in\mathcal{N}_i}B_{ij}\sin\left(\delta_i-\vartheta_j\right)}{M_i}. \tag{36}$$

By making use of both (33) and (36) and exploiting basic algebraic relations, an estimate $\hat{f}_{g_i}$ for f_{g_i} can be obtained as follows.

$$\hat{f}_{g_i} = M_i\big(v_{g_i}-\tilde{v}_{g_i}\big). \tag{37}$$

Figure 1 shows a schematic of the proposed solution to tackle communication attacks for the generator observers.

4.2. Load Observer Communication Attack Reconstruction

The same ideas applied in Section 4.1 will be now used to reconstruct communication attacks at the level of each load observer. Since the procedure is similar to Section 4.1, only a sketch will be provided. Suppose that each super-twisting-like sliding mode observer for the load in the form of (26) receives the corrupted measurements gathered by the neighbouring (generator and load) nodes and the effect of the load disturbance is cancelled by an attack signal. This means that

$$\begin{aligned}
\Omega_i &\triangleq \sum_{j\in\mathcal{M}_i}B_{ij}\sin\Big(y_{l_i}-y_{g_j}\Big)+\sum_{k\in\mathcal{O}_i}B_{ik}\sin\Big(y_{l_i}-y_{l_k}\Big) \\
m_{l_i} &= \frac{f_{l_i}+\Omega_i}{D_{l_i}}
\end{aligned} \tag{38}$$

Following the same procedure presented in Section 4.1, an estimate for the load disturbance can be obtained as

$$\hat{f}_{l_i} = \tfrac{D_i}{2}\Big(\tilde{\psi}_i-\hat{\psi}_i\Big). \tag{39}$$

where $\tilde{\psi}_i$ is the additional variable of the decentralised observer analogous to $\hat{\psi}_i$.

5. Disturbance Mitigation for Generator Nodes

In this section, the distributed disturbance isolation and reconstruction scheme proposed in Section 3 will be applied to mitigate the effect of the disturbances associated with the generator nodes. It is stated that a PI controller has been designed to stabilise each i-th disturbance-free generator node. The aim of the proposed approach is to mitigate the impact of generator disturbances by making use of both the pre-existing PI controller and the estimate of the generator disturbance. Specifically, consider that the generator input power P_{g_i} (the control input) is the output of a standard PI controller as follows:

$$P_{g_i} = K_{P_i}\Delta\hat{\omega}_{g_i} + K_{I_i}\int_0^t \Delta\hat{\omega}_{g_i}(\tau)d\tau, \tag{40}$$

where K_{P_i} and K_{I_i} are respectively the proportional and the integral gain, which have been tuned (by following standard rules, for example as in Kundur et al. (1994)), to asymptotically steer to zero the frequency deviation in each i-th disturbance-free generator node. The control input in (40) is modified as follows:

$$\overline{P}_{g_i} = P_{g_i} - \hat{f}_{g_i}, \tag{41}$$

in which the disturbance estimate $\hat{f}_{g_i}$ is added. It is assumed in the present approach that the expression for $\overline{P}_{g_i}$ in (41) holds only after the attainment of the sliding motion in the system in equations (6)-(7), which takes place in a finite time. The resulting controlled generator dynamics are given by

$$\begin{array}{rcl} \dot{\delta}_i & = & \Delta\omega_{g_i} \\ M_i\Delta\dot{\omega}_{g_i} & = & K_{P_i}\Delta\hat{\omega}_{g_i} + K_{I_i}\int_0^t \Delta\hat{\omega}_{g_i}(\tau)d\tau \\ & & -\sum_{j\in\mathcal{N}_i} B_{ij}\sin(\delta_i - \vartheta_j) \\ & & -D_{g_i}\Delta\omega_{g_i} + f_{g_i} - \hat{f}_{g_i} \\ y_{g_i} & = & \delta_i. \end{array} \tag{42}$$

According to the developments in Section 3, it is apparent that the effect of the generator disturbances is compensated, since $\hat{f}_{g_i}$ asymptotically tends to f_{g_i}. Therefore, in the presence of the disturbance mitigation strategy in (41), the pre-existing PI controller gains can still be employed. As a result, $\Delta\omega_{g_i}$ asymptotically tends to zero.

Remark 5. *The adopted distributed disturbance mitigation strategy acts on each generator node only after the finite time convergence of the error dynamics in* (19) *to the origin. During this transient, which only takes place when the sliding mode is lost, i.e. conceptually only once at the initial onset of the disturbance action, the so-called primary load-frequency control (whose control signal is equal to $-D_{g_i}\Delta\omega_{g_i}$) ensures that, in spite of the presence of a bounded disturbance, the frequency deviation remains bounded (Kundur et al., 1994).*

6. Simulation Results

In this section, the performance of the proposed scheme is evaluated by using the IEEE 39 bus benchmark (Hiskens, 2013), (Moeini et al., 2015). This power network, which has been used in other relevant works for assessment purposes, is composed of 10 generator nodes and 29 load buses, as shown in the schematic in Figure 2.

The power network with the estimation scheme has been simulated in a *Matlab-Simulink R2018a* environment, using the integration method *Ode1* (Euler method) with a fixed integration step size equal to $\tau_{\text{Euler}} = 10^{-4}$ seconds. This choice of the sampling time is also acceptable from a practical perspective, as illustrated in (Gungor et al., 2012), where the latency ranges for the wide-area monitoring schemes for smart power systems have been presented. The filter time constant τ_i in (17) is chosen equal to 0.01 seconds. This tuning is compatible with the selected numerical Matlab solver Ode1 (Euler method), which is characterised by the fixed integration step size τ_{Euler}. It yields $\tau_i >> \tau_{\text{Euler}}$, which is acceptable from the software implementation viewpoint of the proposed observers. The power network is at steady state for $0 < t < 1$ seconds, which means that the power generation is equal to the consumption amongst the nodes At the time instant $t = 1$ seconds, a disturbance of 30 MW affects the 2-nd generator node, whilst at the time instant $t = 2$ seconds, a disturbance of 33 MW acts on the 4-th, 12-th, and 20-th load node. Note that these

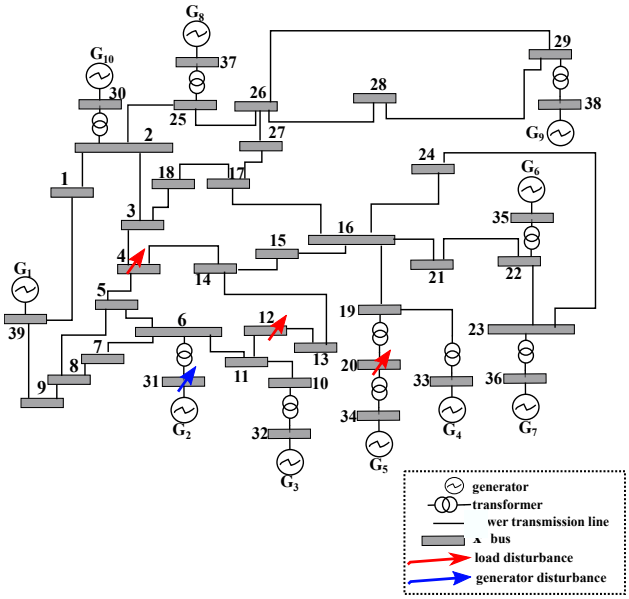

Figure 2: A schematic of the IEEE 39 bus power network comprising 10 generator nodes and 29 load nodes.

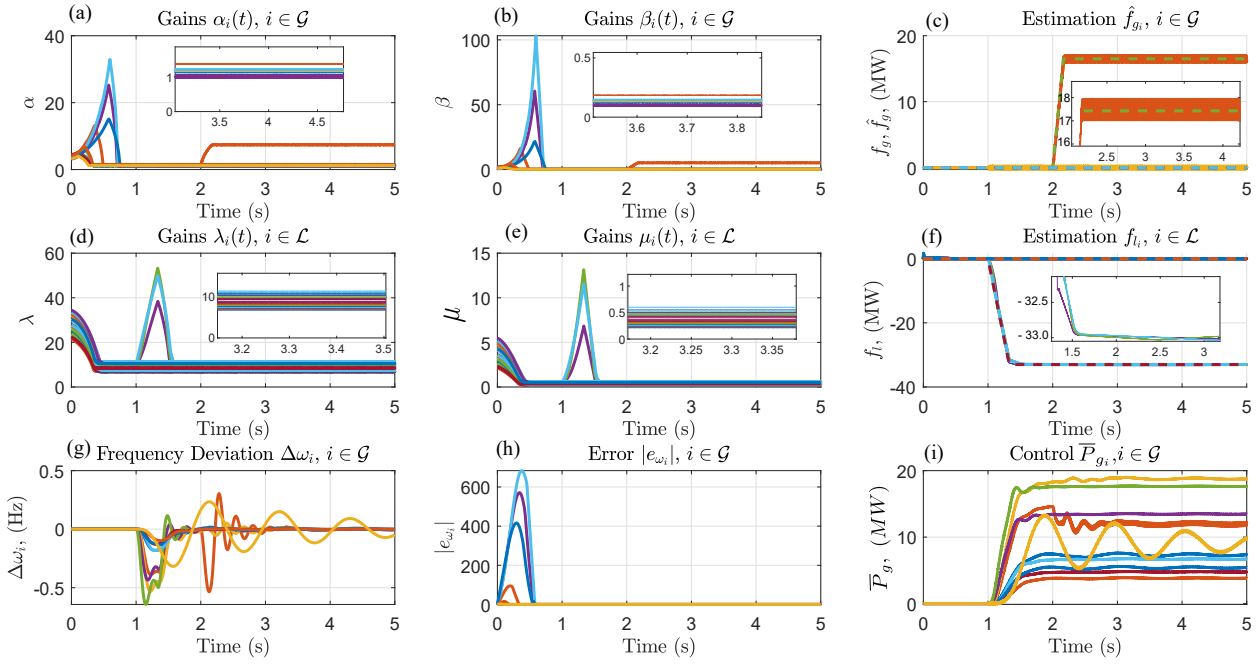

Figure 3: Time histories of (a): the gains $\alpha_i(t)$ in each generator adaptive super-twisting observer; (b) the gains $\beta_i(t)$ in each generator adaptive super-twisting observer; (c) time evolution of the disturbances in the generator nodes; (d) the gains $\lambda_i(t)$ in each load adaptive super-twisting observer; (e) the gains $\mu_i(t)$ in each load adaptive super-twisting observer; (e) time evolution of the frequency deviations and their estimates.

kinds of disturbances can be considered in practice as unregulated generations and consumptions in power systems. The proposed distributed estimation scheme displays the following features:

- As shown in Figure 3-(h), it is possible to dynamically track the evolution of the frequency deviation of each generator node, both at steady state and during the transient due to the disturbances.
- A transient can be noted during the first seconds, which is due to the reaching of the sliding motion, (see Figure 3-(h)).
- The proposed scheme displays the capability of tracking both the generator disturbance and load disturbance, (Figure 3-(c) and Figure 3-(f)).
- The input power at each generator node is regulated according to (41) in a decentralised fashion, by using the local estimate of the frequency deviation and the local generator disturbance reconstruction. From Figure 3-(i) it is possible to note that that all the 10 generator input powers increase, thus asymptotically bringing the frequency deviation back to zero in each generator.
- The adaptive gains for all the observer automatically increase and decrease to deal with the magnitude of the disturbances/attacks while avoiding the gain overestimation, as shown in Figure 3-(a), (b), (d), and (e).

7. Conclusions

In the paper an adaptive distributed estimation scheme has been presented capable of isolating and reconstructing simultaneous disturbances and attacks affecting power networks. Relying on a local exchange of information about the system, it has been possible to design a network of adaptive super-twisting sliding mode observers connected in a distributed fashion. The time-varying gains of the observer are tuned according to a recently proposed dual-layer adaptation law for the super-twisting sliding mode architecture. A disturbance mitigation strategy has been also proposed at each generator node utilising the disturbance estimates. Numerical simulations have been included to assess the performance of the proposed distributed scheme.

Appendix A. Proof of Proposition 1

Consider a candidate Lyapunov function for the system in (19) of the form

$$\begin{aligned} V(t,e_{\delta_i},\bar{e}_{\omega_i}) &= p_{1_i}L_{g_i}(t)|e_{\delta_i}| \\ &\quad +2p_{2_i}L_{g_i}(t)^{1/2}\bar{e}_{\omega_i}\text{sign}(e_{\delta_i})|e_{\delta_i}|^{1/2}+p_{3_i}\bar{e}_{\omega_i}^2 \end{aligned} \tag{A.1}$$

where $p_{1_i}, p_{3_i} > 0$ and $p_{2_i}^2 < p_{1_i}p_{3_i}$. Employing the notation

$$x_i = \text{col}(x_{1_i}, x_{2_i}) := \text{col}(L_{g_i}(t)^{1/2}\text{sign}(e_{\delta_i})|e_{\delta_i}|^{1/2}, \bar{e}_{\omega_i}) \tag{A.2}$$

The Lyapunov function $V(t,e_{\delta_i},\bar{e}_{\omega_i})$ in (A.1) can be written as $V = x_i^T P_i x_i$ where the symmetric positive definite matrix

$$P_i = \begin{bmatrix} p_{1_i} & p_{2_i} \\ p_{2_i} & p_{3_i} \end{bmatrix} \tag{A.3}$$

Since $L_{g_i}(t)$ is bounded and $L_{g_i}(t) > l_{0_i} > 0$, then exploiting the positivity of P_i implies $V(t,e_{\delta_i},\bar{e}_{\omega_i})$ is positive definite with respect to $(e_{\delta_i},\bar{e}_{\omega_i})$, continuous and radially unbounded. The expression for the time derivative $\dot{V}$ will now be obtained in terms of (x_{1_i},x_{2_i}), which therefore requires expressions for $\dot{x}_{1_i}$ and $\dot{x}_{2_i}$. From (19), for $e_{\delta_i} \neq 0$, x_{1_i} from

(A.2) satisfies

$$\begin{aligned}\dot{x}_{1_i} &= \frac{\sqrt{L_{g_i}(t)}}{2|e_{\delta_i}|^{1/2}}\Big(-\alpha_i(t)\text{sign}(e_{\delta_i})|e_{\delta_i}|^{1/2}+\overline{e}_{\omega_i}+\Phi_{g_i}(\cdot)\Big)\\ &\quad+\frac{\dot{L}_{g_i}(t)}{2\sqrt{L_{g_i}(t)}}\text{sign}(e_{\delta_i})|e_{\delta_i}|^{1/2}\\ &= -\frac{\alpha_i(t)}{2|e_{\delta_i}|^{1/2}}x_{1_i}+\frac{\sqrt{L_{g_i}(t)}}{2|e_{\delta_i}|^{1/2}}\overline{e}_{\omega_i}+\frac{\sqrt{L_{g_i}(t)}}{2|e_{\delta_i}|^{1/2}}\Phi_{g_i}(\cdot)\\ &\quad+\frac{\dot{L}_{g_i}(t)}{2\sqrt{L_{g_i}(t)}}\text{sign}(e_{\delta_i})|e_{\delta_i}|^{1/2}\\ &= -\frac{\alpha_i(t)}{2|e_{\delta_i}|^{1/2}}x_{1_i}+\frac{\sqrt{L_{g_i}(t)}}{2|e_{\delta_i}|^{1/2}}x_{2_i} \qquad (A.4)\end{aligned}$$

since by the definition of $\Phi_{g_i}(\cdot)$ in (12)

$$\frac{\sqrt{L_{g_i}}(t)}{2|e_{\delta_i}|^{1/2}}\Phi_{g_i}(\cdot)+\frac{\dot{L}_{g_i}(t)}{2\sqrt{L_{g_i}}(t)}\text{sign}(e_{\delta_i})|e_{\delta_i}|^{1/2}=0 \qquad (A.5)$$

Furthermore when $e_{\delta_i}\neq 0$, x_{2_i} from (A.2) satisfies

$$\begin{aligned}\dot{x}_{2_i} &= \frac{1}{|e_{\delta_i}|^{1/2}}\Big(-\beta_i(t)\text{sign}(e_{\delta_i})|e_{\delta_i}|^{1/2}-|e_{\delta_i}|^{1/2}\frac{f_{g_i}}{M_i}\Big)\\ &= \frac{\sqrt{L_{g_i}(t)}}{|e_{\delta_i}|^{1/2}}\Big(-\frac{\beta_i(t)}{L_{g_i}(t)}x_{1_i}-\tilde{f}_i\Big) \qquad (A.6)\end{aligned}$$

where the (re-defined) uncertainty in (A.6) is given by

$$\tilde{f}_i=\frac{|e_{\delta_i}|^{1/2}}{\sqrt{L_{g_i}(t)}}\frac{f_{g_i}}{M_i} \qquad (A.7)$$

Since $|x_{1_i}|=\sqrt{L_{g_i}(t)}|e_{\delta_i}|^{1/2}$ it follows from (A.7) that the re-defined uncertainty satisfies

$$|\tilde{f}_i|\leq\frac{|f_{g_i}/M_i|}{L_{g_i}(t)}|x_{1_i}| \qquad (A.8)$$

Since by assumption $|f_{g_i}/M_i|<L_{g_i}(t)$, it follows that $|\tilde{f}_i|\leq|x_{1_i}|$ i.e the uncertainty $\tilde{f}_i$ lies in the sector $[\ -1\quad 1\ ]$. Using the definitions of $\alpha_i(t)$ and $\beta_i(t)$ in (8)-(9) it follows that (A.4) and (A.6) can be written in concise form as

$$\dot{x}_i=\frac{L_{g_i}(t)}{|x_{1_i}|}\Big(A_{0_i}x_i-B_{0_i}\tilde{f}_i\Big),\quad x_{1_i}\neq 0 \qquad (A.9)$$

where

$$A_{0_i}=\begin{bmatrix}-\frac{1}{2}\alpha_{0_i} & \frac{1}{2}\\ -\beta_{0_i} & 0\end{bmatrix}\quad B_{0_i}=\begin{bmatrix}0\\1\end{bmatrix} \qquad (A.10)$$

Therefore along any solution of (19), when $e_{\delta_i}\neq 0$,

$$\dot{V}=\frac{L_{g_i}(t)}{|x_{1_i}|}\Big(x_i^T(P_iA_{0_i}+A_{0_i}^TP)x_i-2x_i^TP_iB_{0_i}\tilde{f}_i\Big) \qquad (A.11)$$

where x_i is defined in (A.2). Applying Young's inequality to (A.11) yields

$$\dot{V} \leq \frac{L_{g_i}(t)}{|x_{1_i}|}\left(x_i^T(P_iA_{0_i}+A_{0_i}^TP_i+P_iB_{0_i}B_{0_i}^TP_i)x_i+|\tilde{f}_i|^2\right) \tag{A.12}$$

It follows the state component $x_{1_i}=C_{0_i}x_i$, if $C_{0_i}=\begin{bmatrix}1 & 0\end{bmatrix}$. Then since $|\tilde{f}_i|\leq|x_{1_i}|$, it follows from (A.12) that

$$\begin{aligned}\dot{V} &\leq \frac{L_{g_i}(t)}{|x_{1_i}|}\left(x_i^T(P_iA_{0_i}+A_{0_i}^TP_i+P_iB_{0_i}B_{0_i}^TP_i)x_i+|x_{1_i}|^2\right)\\ &= \frac{L_{g_i}(t)}{|x_{1_i}|}x_i^T\left(P_iA_{0_i}+A_{0_i}^TP_i+P_iB_{0_i}B_{0_i}^TP+C_{0_i}^TC_{0_i}\right)x_i\\ &\leq -\varepsilon_{0_i}\frac{L_{g_i}(t)}{|x_{1_i}|}V\end{aligned} \tag{A.13}$$

It follows from Rayleigh's inequality that $V>\lambda_{min}(P_i)\|x_i\|^2>\lambda_{min}(P_i)|x_{1_i}|^2$ and therefore

$$\sqrt{V}>\sqrt{\lambda_{min}(P_i)}|x_{1_i}|$$

Since by definition $L_{g_i}(t)>l_{0_i}$ where l_{0_i} is a positive scalar, from (A.13)

$$\dot{V}\leq-\varepsilon_{0_i}\frac{L_{g_i}(t)}{|x_{1_i}|}V\leq-\frac{\varepsilon_{0_i}l_{0_i}V}{|x_{1_i}|}\leq-\kappa_i\sqrt{V} \tag{A.14}$$

where the positive scalar $\kappa_i=\varepsilon_{0_i}l_{0_i}\sqrt{\lambda_{min}(P_i)}$. It follows from the arguments above that along the solution of (19), whenever $e_{\delta_i}\neq0$, $\dot{V}\leq-\kappa_i\sqrt{V}$. The function V defined in (A.1) is continuous and differentiable except on the set $\mathcal{S}=\{(e_{\delta_i},\overline{e}_{\omega_i}):e_{\delta_i}=0\}$. The trajectories of (19) cannot stay on $\mathcal{S}$ since any point in this set takes the form $(0,\overline{e}_{\omega_i})$ where $\overline{e}_{\omega_i}\neq0$, and from (19), $\dot{e}_1=\overline{e}_{\omega_i}\neq0$. Consequently V is a continuous decreasing function and therefore from the 'Lyapunov' result for differential inclusions (Deimling, 2011), the equilibrium point $(e_{\delta_i},\overline{e}_{\omega_i})=(0,0)$ is reached in finite time. Substituting for $e_{\delta_i}=\overline{e}_{\omega_i}=0$ in (19) it follows that $\dot{e}_1=0$ in finite time. □

Appendix B. Proof of Proposition 2

Define a new variable

$$e_i(t)=q_ia_{1_i}/(\eta_i\beta_{0_i})-r_{g_i}(t) \tag{B.1}$$

where the scalar $q_i>1$ and represents a safety margin to guarantee $|\frac{d}{dt}|(v_{g_i}(t))||<q_ia_{1_i}$, where a_{1_i} is a positive unknown constant representing the upper-bound for $|\dot{f}_{g_i}|/M_i$. From the definition of $e_i(t)$ and the expression for $\dot{r}_{g_i}(t)$ from (14), it follows that

$$\dot{e}_i(t)=-\dot{r}_{g_i}(t)=-\gamma_i\left|\varphi_{g_i}(t)\right| \tag{B.2}$$

Arguing as in Utkin and Poznyak (2013) the variable $\varphi_{g_i}(t)$ from (15) evolves according to

$$\dot{\varphi}_{g_i}(t)=\dot{l}_{g_i}(t)-\frac{1}{\eta_i\beta_{0_i}}\frac{d}{dt}|v_{g_i}(t)| \tag{B.3}$$

Consequently from (11)

$$\dot{\varphi}_{g_i}(t)=-\underbrace{(r_{0_i}+q_ia_{1_i}/(\eta_i\beta_{0_i})-e_i(t))}_{\rho_{g_i}(t)}\operatorname{sign}(\varphi_{g_i}(t))-1/(\eta_i\beta_{0_i})\phi_{g_i} \tag{B.4}$$

where $\phi_{g_i}(t) = \frac{d}{dt}|v_{g_i}(t)|$ and $|\phi_{g_i}(t)| < q_i a_{1_i}$ where $q_i > 1$. The dynamical system formed from the variables $\varphi_{g_i}(t)$ and $e_i(t)$, evolving according to (B.2) and (B.4), will now be analysed using the Lyapunov function candidate

$$V(\varphi_{g_i}(t), e_i(t)) = \frac{1}{2}\varphi_{g_i}^2(t) + \frac{1}{2\gamma_i}e_i^2(t) \tag{B.5}$$

From (B.4) it follows that

$$\begin{aligned}\dot{\varphi}_{g_i}(t)\varphi_{g_i}(t) &\leq \varphi_{g_i}\dot{l}_{g_i}(t) + |\varphi_{g_i}(t)|\frac{q_i a_{1_i}}{\eta_i\beta_{0_i}} \\ &= -r_{0_i}|\varphi_{g_i}(t)| - r_{g_i}(t)|\varphi_{g_i}(t)| + |\varphi_{g_i}(t)|\frac{q_i a_{1_i}}{\eta_i\beta_{0_i}} \\ &= -r_{0_i}|\varphi_{g_i}(t)| + e_i(t)|\varphi_{g_i}(t)| \end{aligned} \tag{B.6}$$

from the definition of $e_i(t)$ in (B.1). Therefore the derivative of (B.5) along the trajectories of $\varphi_{g_i}(t)$ and $e_i(t)$ satisfies

$$\begin{aligned}\dot{V} &\leq -r_{0_i}|\varphi_{g_i}(t)| + |\varphi_{g_i}(t)|e_i(t) - \tfrac{1}{\gamma_i}e_i(t)\dot{r}_{g_i}(t) \\ &= -r_{0_i}|\varphi_{g_i}(t)| + |\varphi_{g_i}(t)|e_i(t) - |\varphi_{g_i}(t)|e_i(t) \\ &= -r_{0_i}|\varphi_{g_i}(t)| \end{aligned} \tag{B.7}$$

Since $\dot{V} \leq 0$, and $V(\varphi_{g_i}(t), e_i(t))$ is radially unbounded, it follows that both $e_i(t)$ and $\varphi_{g_i}(t)$ remain bounded. Consequently since $r_{g_i}(t) = q_i a_{1_i}/(\eta_i\beta_{0_i}) - e_i(t)$ it follows that $r_{g_i}(t)$ remains bounded since $e_i(t)$ is bounded. Likewise since $|L_{g_i}(t)| \leq |\varphi_{g_i}(t)| + q_i a_{1_i}/(\eta_i\beta_0) + \iota_{g_i}$ and $\varphi_{g_i}(t)$ is bounded, the gain $L_{g_i}(t)$ remains bounded. Since $e_i(t)$ and $\varphi_{g_i}(t)$ remain bounded, from (B.4), the derivative $\dot{\varphi}_{g_i}(t)$ remains bounded and therefore $\varphi_{g_i}(t)$ is absolutely continuous. It follows from (B.7) that

$$r_{0_i}\int_0^t |\varphi_{g_i}(t)|dt \leq V(0) - V(t) < V(0)$$

where $|\varphi_{g_i}(t)|$ is absolutely continuous. Therefore from Barbalat's Lemma, $\varphi_{g_i}(t) \to 0$ as $t \to \infty$. Consequently there exists a finite time t_0 such that $|\varphi_{g_i}(t)| \leq \iota_{g_i}/2$ for all time $t > t_0$ (where ι_{g_i} is from the definition of $\varphi_{g_i}(t)$ in (15). From the definition of φ_{g_i} in (15) it follows

$$|\varphi_{g_i}(t)| = \left|L_{g_i}(t) - \frac{1}{\eta_i\beta_{0_i}}|v_{g_i}(t)| - \iota_{g_i}\right| < \iota_{g_i}/2$$

and thus

$$L_{g_i}(t) - \frac{1}{\eta_i\beta_{0_i}}|v_{g_i}(t)| - \iota_{g_i} > -\iota_{g_i}/2$$

Since by definition $\eta_i\beta_{0_i} < 1$, it follows the gain $L_{g_i}(t)$ satisfies

$$L_{g_i}(t) > \frac{1}{\eta_i\beta_{0_i}}|v_{g_i}(t)| + \frac{\iota_{g_i}}{2} > |v_{g_i}(t)| = |f_{g_i}/M_i| \tag{B.8}$$

From (B.8) it follows that the claim in the proposition statement is proved. □

References

Deimling, K., 2011. Multivalued differential equations. volume 1. Walter de Gruyter.

Dorfler, F., Bullo, F., 2013. Kron reduction of graphs with applications to electrical networks. IEEE Transactions on Circuits and Systems I: Regular Papers 60, 150–163.

Edwards, C., Shtessel, Y., 2016. Adaptive dual-layer super-twisting control and observation. International Journal of Control 89, 1759–1766.

Edwards, C., Spurgeon, S., 1998. Sliding mode control: theory and applications. Crc Press.

Gonzalez, T., Moreno, J.A., Fridman, L., 2011. Variable gain super-twisting sliding mode control. IEEE Transactions on Automatic Control 57, 2100–2105.

Gungor, V.C., Sahin, D., Kocak, T., Ergut, S., Buccella, C., Cecati, C., Hancke, G.P., 2012. A survey on smart grid potential applications and communication requirements. IEEE Transactions on industrial informatics 9, 28–42.

Hiskens, I., 2013. IEEE PES task force on benchmark systems for stability controls. Technical Report .

Kundur, P., Balu, N.J., Lauby, M.G., 1994. Power system stability and control. volume 7. McGraw-hill New York.

Li, J., Xu, L., Zhang, Z., 2005. An adaptive sliding-mode observer for induction motor sensorless speed control. IEEE Transactions on Industry Applications 41, 1039–1046.

Liu, J., Laghrouche, S., Harmouche, M., Wack, M., 2014. Adaptive-gain second-order sliding mode observer design for switching power converters. Control Engineering Practice 30, 124–131.

Moeini, A., Kamwa, I., Brunelle, P., Sybille, G., 2015. Open data IEEE test systems implemented in simpowersystems for education and research in power grid dynamics and control, in: Proc. of 50- th International Universities Power Engineering Conference (UPEC), Staffordshire University, UK, September 2015. pp. 1–6.

Moreno, J.A., Negrete, D.Y., Torres-González, V., Fridman, L., 2016. Adaptive continuous twisting algorithm. International Journal of Control 89, 1798–1806.

Nateghi, S., Shtessel, Y., Edwards, C., Barbot, J.P., 2019. Cyber-attacks and faults reconstruction using finite time convergent observation algorithms: Electric power network application, in: Control Theory in Engineering. IntechOpen.

Pappachen, A., Fathima, A.P., 2017. Critical research areas on load frequency control issues in a deregulated power system: A state-of-the-art-of-review. Renewable and Sustainable Energy Reviews 72, 163–177.

Pasqualetti, F., Dorfler, F., Bullo, F., 2015. Control-theoretic methods for cyberphysical security: Geometric principles for optimal cross-layer resilient control systems. IEEE Control Systems Magazine 35, 110–127.

Phadke, A.G., Thorp, J.S., 2017. Phasor measurement units and phasor data concentrators, in: Synchronized Phasor Measurements and Their Applications. Springer, pp. 83–109.

Rinaldi, G., Cucuzzella, M., Ferrara, A., 2017. Third order sliding mode observer-based approach for distributed optimal load frequency control. IEEE Control Systems Letters 1, 215–220.

Rinaldi, G., Menon, P.P., Edwards, C., Ferrara, A., 2018a. Distributed super-twisting sliding mode observers for fault reconstruction and mitigation in power networks, in: Proc. 57th IEEE Conference on Decision and Control, Miami, Florida, USA, December 2018.

Rinaldi, G., Menon, P.P., Edwards, C., Ferrara, A., 2018b. Sliding mode based dynamic state estimation for synchronous generators in power systems. IEEE Control Systems Letters 2, 785–790.

Rinaldi, G., Menon, P.P., Edwards, C., Ferrara, A., 2020. Design and validation of a distributed observer-based estimation scheme for power grids. IEEE Transactions on Control Systems Technology 28, 680–687.

Saoudi, K., Harmas, M., 2014. Enhanced design of an indirect adaptive fuzzy sliding mode power system stabilizer for multi-machine power systems. International Journal of Electrical Power & Energy Systems 54, 425–431.

Sauer, P.W., Pai, M., Chow, J.H., 2017. Power System Dynamics and Stability: With Synchrophasor Measurement and Power System Toolbox. John Wiley & Sons.

Shayeghi, H., Shayanfar, H., Jalili, A., 2009. Load frequency control strategies: A state-of-the-art survey for the researcher. Energy Conversion and Management 50, 344–353.

Shen, Q., Shi, P., Wang, S., Shi, Y., 2019a. Fuzzy adaptive control of a class of nonlinear systems with unmodeled dynamics. International Journal of Adaptive Control and Signal Processing 33, 712–730.

Shen, Q., Shi, P., Zhu, J., Zhang, L., 2019b. Adaptive consensus control of leader-following systems with transmission nonlinearities. International Journal of Control 92, 317–328.

Shi, P., Shen, Q., 2017. Observer-based leader-following consensus of uncertain nonlinear multi-agent systems. International Journal of Robust and Nonlinear Control 27, 3794–3811.

Tebianian, H., Jeyasurya, B., 2015. Dynamic state estimation in power systems: Modeling, and challenges. Electric Power Systems Research 121, 109–114.

Tsai, S.B., Xue, Y., Zhang, J., Chen, Q., Liu, Y., Zhou, J., Dong, W., 2017. Models for forecasting growth trends in renewable energy. Renewable and Sustainable Energy Reviews 77, 1169–1178.

Tursini, M., Petrella, R., Parasiliti, F., 2000. Adaptive sliding-mode observer for speed-sensorless control of induction motors. IEEE Transactions on Industry Applications 36, 1380–1387.

Utkin, V.I., Poznyak, A.S., 2013. Adaptive sliding mode control with application to super-twist algorithm: Equivalent control method. Automatica 49, 39–47.

Wang, W., Lu, Z., 2013. Cyber security in the smart grid: Survey and challenges. Computer Networks 57, 1344–1371.

Zhao, C., Mallada, E., Dörfler, F., 2015. Distributed frequency control for stability and economic dispatch in power networks, in: Proc. American Control Conference, Chicago, IL, USA, July 2015. pp. 2359–2364.